Supplemental Data

Supplemental Figure 1. Selected clinical parameters differentially detected in subgroups of COVID-19 patients with different clinical severity. (A): STROBE Flow chart of the study showing patient recruitment and stratification according to clinical severity (B): Box and Whiskers plots representing clinical values of PaFiO2, IL-6, procalcitonin, IFNα and C Reactive Protein detected in the blood of total number of COVID-19 patients or patients stratified into mild (G1; n=19), severe (SEV, G2; n=21) and critical (CRIT, G3; n=24) clinical status defined according to the criteria detailed in Supplemental Table 1. Values present in non-COVID-19 controls (NC; n=22) were included when available. Error bars represent maximum and minimum values. Statistical significance of differences in clinical values across the study groups were calculated using a Kruskal Wallis and Dunn´s post-hoc test for multiple comparisons. *p<0.05; **p<0.01; ***p<0.001; ****p<0.0001. (C): Time since hospital admission (left) and symptoms duration (right) at the time of sample collection for the three mentioned subgroups of COVID-19 patients. Statistical significance was calculated using a Kruskal Wallist and Dunn´s post-hoc tests. *p<0.05; ***p<0.001.

Supplemental Figure 2. Flow cytometry characterization of myeloid cell subsets from COVID-19 patients. (A): Flow cytometry gating strategy showing Monocyte (Mo), conventional (cDC) and plasmacytoid DC (pDC) and granulocyte characterization in the blood from a representative patient of our study cohorts. $CD14^+$ Lineage ($CD3^-$ $CD19^-$ $CD20^-$ $CD56^-$) negative Mo subsets were defined by CD14 and CD16 expression levels. Granulocytes were identified as large $CD16^{hi}$ $CD14^{lo/-}$ $HLADR^-$ cells. cDC subsets were identified as $CD14^-$ Lin^- $HLA\text{-}DR^+$ big

cells differing on CD1c and CD141 expression. Finally, pDCs were defined as $CD14^{-}Lin^{-}CD11c^{-}$ $HLADR^{+}$ $CD123^{hi}$ lymphocytes. (B-C): Box and whiskers plots reflecting proportions of granulocytes (B) and ratios of frequencies between Transitional Mo/$CD1c^{+}$ cDC and Granulocyte/ $CD1c^{+}$ cDCs (C) present in the blood of non-COVID-19 control individuals (n=22) compared with either total COVID-19 patients included in the study or patients stratified into mild (G1; n=19), severe (SEV, G2; n=21) and critical (CRIT, G3; n=24). Error bars represent maximum and minimum values. Statistical differences between patient groups were calculated using a Kruskal Wallis test followed by a Dunn´s post hoc-test for multiple comparisons. *$p<0.05$.

Supplemental Figure 3. Analysis of Absolute numbers of myeloid subsets in COVID-19 cohort groups and stratification of critical patients based on microbial superinfection. (A-C): Box and Whiskers plots representing absolute numbers of indicated myeloid cell populations present in the blood of non-COVID-19 (NC; n=22) control individuals versus either total COVID-19 patients included in the study or patients stratified into groups according to mild (G1; n=19), severe (SEV, G2; n=21) and critical (CRIT, G3; n=22) clinical status as shown in Supplemental Table 1. Median of values is shown. Error bars represent maximum and minimum values. (B) Box and Whiskers plots representing relative (left plots) and absolute (right plots) numbers for all cell populations from NC controls versus total critical G3 COVID-19 patients or stratified based on the presence of microbial superinfection (Sup. Inf) in the lung (n=8), both lung and blood (Bd) or unine (Ur) (n=2), or only in Bd/Ur (n=6) or that did not present super infection (No Sup. Inf; n=4). Median of values is shown. Error bars represent maximum and minimum values. Statistical significance of differences between all patient groups (A) or COVID-19 patients compared to non-

COVID-19 controls (NC) in (B) was calculated using a Kruskal Wallis test followed by a Dunn´s post hoc-test for multiple comparisons. *p<0.05; **p<0.01; ***p<0.001; ****p<0.0001.

Supplemental Figure 4. Analysis of frequencies of circulating myeloid subsets in COVID-19 after stratification of critical patients based on days at ICU. Box and whiskers plots reflecting frequencies of the indicated circulating myeloid subsets in critical G3 COVID-19 patients stratified by time since hospital admission (< 6 days, n=13; > 6 days, n=11) and compared to mild (G1; n=19), severe (SEV, G2; n=21) and total critical (CRIT, G3; n=24) patients. Error bars represent maximum and minimum values. Statistical significance of differences between patient groups was calculated using a Kruskal Wallis test followed by a Dunn´s post hoc-test for multiple comparisons. *p<0.05; **p<0.01; ***p<0.001; ****p<0.0001.

Supplemental Figure 5. Correlation of frequencies of circulating myeloid cell subsets with IL-6 and inflammatory marker plasma levels. Spearman correlations between IL-6 plasma levels (A) or inflammatory clinical values (B-C) and percentages of the indicated myeloid cell subsets in the blood of COVID-19 patients. Spearman P and R values are shown in the upper right corner of the plot.

Supplemental Figure 6. tSNE representation of activation status of myeloid cell subsets and correlation between frequencies in the blood and inflammatory molecule plasma levels. (A): tSNE plots displaying heatmaps of CD40 mean of fluorescence intensity (MFI) in different cell clusters specified in Figure 1 from Non-COVID-19 (NC) control individuals (left, n=15) and (n=34) total COVID-19 patients or stratified based on clinical severity on G1 (MILD), G2 (SEV)

and G3 (CRIT) subgroups. Red arrows highlight areas where differences across patient groups can be appreciated. (B): Representative flow cytometry dot plots showing expression of CD40 on gated CD1c+ cDC, CD141+ cDCs and CD123+ pDC from non-COVID19 controls (NC), mild G1, severe G2 and critical G3 patients. FMO controls for each cell subset are included for comparison purposes. (C): CD40 Mean of fluorescence intensity (MFI) on the indicated myeloid cell populations present in the blood of non-COVID-19 controls (NC; n=22) individuals versus either total COVID-19 patients included in the study or patients stratified in mild (G1; n=19), severe (SEV, G2; n=21) and critical (CRIT, G3; n=24) clinical characteristics specified in Supplemental Table 1. (D-E): Spearman correlation between CD40 MFI on the indicated myeloid cell subsets and their frequency in blood (D) or IL-6 plasma levels (E). Spearman P and R values are shown in the upper right corner of the plot. Statistical significance of each cell subset between each patient subgroup was tested using a two tailed Mann Whitney test. (F): Spearman correlations between procalcitonin (PCT) levels in plasma and CD40 mean fluorescence intensity (MFI) on CD1c+ cDCs, classical (C), transitional (T) and non-classical (NC) Mo. Spearman P and R values are shown in the upper right corner of the plot.

Supplemental Figure 7. Characterization of myeloid cells present in bronchoscopy infiltrates from COVID-19 patients with ARDS. (A): Dot plots representing proportions of $CD45^+$ hematopoietic cells present in bronchoscopy samples obtained from COVID-19 patients (n=23) with severe ARDS and requiring IMV at hospital´s ICU. Associations with clinical parameters in samples with frequencies of CD45+ hematopoietic cell superior or inferior to 50% are shown below. Median values are highlighted with a line. (B): Flow cytometry analyses of myeloid cell subsets hematopoietic infiltrates from bronchoscopy compared with bronchoalveolar lavage

(BAL) from the same COVID-19 severe patient. Two representative examples are shown. (C): Quantification of proportions of the indicated myeloid population in the BAL and bronchoscopy (Brc.) from the two patients shown in (B). (D-E): Box and Whiskers plots representing percentages (D,left) and CD40 Mean of Fluorescence Intensity (MFI D, right) corresponding to the indicated cell populations in the hematopoietic $CD45^+$ infiltrate present in bronchoscopy mucus samples from severe COVID-19 patients (n=20) presenting ARDS and receiving IMV at ICU and stratified by detection of microbial superinfection only in the lung (Lg; n=10), both in lung and Blood or Urine (Lg+B/U; n=3) or only in the blood or urine (B/U; n=7) or time of sample collection since ICU admission (E) (< 6 days, n=14; > 6 days, n=6). Median are highlighted and error bars represent maximum and minimum datapoint. Statistical differences between proportions of cell populations within the same infiltrates were calculated using a two-tailed matched pairs Mann Whitney test and Bonferroni multiple comparison correction. (F): Frequencies of CD14lo/-CD16hi HLA-DR- granulocytes on the blood and paired bronchoscopy samples from critical COVID-19 patients. Statistical differences were calculated using a two-tailed matched pairs Wilcoxon test. **, $p<0.01$; ***; $p<0.001$.

Supplemental Figure 8. Characterization of effector $CD8^+$ T cells present in bronchoscopy infiltrates from COVID-19 patients with ARDS. (A-B): Percentages of total $CD4^+$ and $CD8^+$ T cells and $CD4^+$T/$CD8^+$T ratios (A) or $CXCR5^+CD38^+$, $CXCR5^+$ $CD38^-$ and $CXCR5^-$ $CD38^+$ (B) from $CD8^+$ T cells in the blood and paired bronchoscopy samples from n=15 COVID-19 patients with ARSD (n=15). Statistical significance was calculated using a two tailed matched pairs Wilcoxon test for differences of the same populations between different tissue localizations (black) or between different cell populations included within the blood (blue) or within the bronchoscopy

(pink) samples. (C-D): Spearman correlations between proportions of $CXCR5^{+}CD38^{+}$, $CXCR5^{+}$ $CD38^{-}$ and $CXCR5^{-}$ $CD38^{+}$ subpopulations of $CD8^{+}$ T cells from bronchoscopy samples from COVID-19 patients and ratios of frequencies between Transitional (T) or non-classic (NC) Mo versus $CD1c^{+}$ cDCs (C) and CD40 MFI of the indicated myeloid populations in bronchoscopy samples (D). Spearman P and R values are shown in the upper right corner of the plot.

Supplemental Acknowledgments for Consortium

REINMUN-COVID group includes:

Cardiology Unit from Hospital Universitario La Princesa

Teresa Alvarado, Pablo Martínez, Francisco Javier de la Cuerda Llorente

Emergency Service from Hospital Universitario La Princesa

Carmen del Arco, Juan Mariano Aguilar, Natalia Villalba, Mónica Negro, Elvira Contreras, Ana del Rey, Cristina Santiago, Manuel Junquera, Raquel Caminero, Francisco Javier Val, Sonia González, Marta Caño, Isabel López, Andrés von Wernitz, Bárbara Retana, Iñigo Guerra, Jorge Sorando, Lydia Chao, María José Cárdenas, Verónica Espiga, Pablo Chicharro, Pedro Rodríguez.

Endocrinology Unit from Hospital Universitario La Princesa

Iñigo Hernando Alday, Miguel Sampedro

ENT

Jorge Prada

Gastroenterology

Eukene Rojo Aldama, Yolanda Real, María Caldas, Sergio Casabona, Aitor Lanas-Gimeno.

Hematology Service

Rafael de la Camara, Angela Figuera Alvárez, Beatriz Aguado.

Hospital Pharmacy

Alberto Morell, Esther Ramírez, Amparo Ibáñez Zurriaga, María Pérez Abanades, Silvia Ruiz García, Tomás Gallego Aranda, María Ruiz, Concepción Martínez Nieto, José María Serra.

Intensive Care Unit from Hospital Universitario La Princesa

Alfonso Canabal, Patricia Albert, Diego A. Rodriguez-Serrano, Judit Iglesias, Fernando Suarez, Juan Antonio Sánchez, Beatriz Abad.

Internal Medicine-Infectious Diseases

Carmen Suarez, Ignacio de los Santos, José María Galván-Roman, Emilia Roy, Pablo Rodríguez-Cortes, Lucio García-Fraile, Jesus Sanz, Eduardo Sanchez, Fernando Moldenhauer, Pedro Casado, Jose Curbelo, Angela Gutierrez, Azucena Bautista, Nuria Ruiz Giménez, Angelica Fernandez, Pedro Parra, Berta Moyano, Ana Barrios, Diego Real de Asua, Beatriz Sanchez, Carmen Saez, Marianela Ciudad.

Immunology Unit from Hospital Universitario La Princesa

Francisco Sánchez-Madrid, Cecilia Muñoz-Calleja, Enrique Martín-Gayo, Arantzazu Alfranca, Javier Aspa, Ana Marcos-Jiménez, Santiago Sánchez-Alonso, Marta Calvet-Mirabent, Ana Alcaraz-Serna, Tamara Mateu-Albero, Ildefonso Sánchez-Cerrillo, Laura Esparcia, Pedro Martínez-Fleta, Celia López-Sanz, Ligia Gabrie, Luciana del Campo Guerola, Elena Fernández, Mª José Calzada, Reyes Tejedor.

Medical Biology Unit from Hospital Universitario La Princesa

Desiré Navas

Microbiology Unit from Hospital Universitario La Princesa

Laura Cardeñoso Domingo, María del Carmen Cuevas Torresano, Diego Domingo García, Teresa Alarcón Cavero, Alicia García Blanco, Alexandra Martín Ramírez, María Auxiliadora Semiglia Chong, Ainhoa Gutiérrez Cobos, Nelly Daniela Zurita Cruz, Arturo Manuel Fraile Torres.

Nephrology Unit from Hospital Universitario La Princesa

Carmen Sanchez-Gonzalez, Antonio Fernádez Perpén

Neurology Unit from Hospital Universitario La Princesa

Carolina Díaz Pérez

Pneumology Unit from Hospital Universitario La Princesa

Julio Ancochea, Tamara Alonso, Pedro Landete, Joan Soriano, Carolina Cisneros, Elena García Castillo, Francisco Javier García Pérez, Rosa María Girón, Celeste Marcos, Enrique Zamora.

Radiology Unit from Hospital Universitario La Princesa

Patricia García García

Rheumatology Unit from Hospital Universitario La Princesa

Santos Castañeda, Rosario García-Vicuña, Isidoro González-Álvaro, Sebastián Rodríguez-García, Carlos Fernández-Díaz, Irene Llorente Cubas, Eva G. Tomero, Noelia García Castañeda, Ana Mª Ortiz, Cristina Valero, Miren Uriarte, Nuria Montes.

EDEPIMIC group includes:

Immunology Unit from Hospital Universitario La Princesa

Francisco Sánchez-Madrid, Cecilia Muñoz-Calleja, Enrique Martín-Gayo, Arantzazu Alfranca, Javier Aspa, Ana Marcos-Jiménez, Santiago Sánchez-Alonso, Ana Alcaraz-Serna, Tamara Mateu-Albero, Ildefonso Sánchez-Cerrillo, Marta Calvet-Mirabent, Laura Esparcia, Pedro Martínez-Fleta, Celia López-Sanz, Ligia Gabrie, Luciana del Campo Guerola, Elena Fernández, Mª José Calzada, Reyes Tejedor.

Pneumology Unit from Hospital Universitario La Princesa

Julio Ancochea, Tamara Alonso, Pedro Landete, Joan Soriano, Carolina Cisneros, Elena García Castillo, Francisco Javier García Pérez, Rosa María Girón, Celeste Marcos, Enrique Zamora.

Rheumatology Unit from Hospital Universitario La Princesa

Santos Castañeda, Rosario García-Vicuña, Isidoro González-Álvaro, Sebastián Rodríguez-García, Carlos Fernández-Díaz, Irene Llorente Cubas, Eva G. Tomero, Noelia García Castañeda, Ana Mª Ortiz, Cristina Valero, Miren Uriarte, Nuria Montes.

International advisor committee:

Maria Montes de Oca (Neumoepidemiology; Caracas, Venezuela); Antonio R Anzueto (pneumology and ICU expert; San Antonio, Texas, USA); Rogelio Pérez Padilla (Pneumoepidemiologist, Ciudad de México, México); Alberto García-Basteiro (Tuberculosis epidemiologist and expert on infectious diseases; Maniça, Mozambique.)

	Healthy	All COVID-19 Blood	G1 Mild COVID-19 Blood	G2 Severe COVID-19 Blood	G3 Critical COVID-19 Blood	G3 Critical COVID-19 Bronch.
Number of patients (n)	**22**	**64**	**19**	**21**	**24**	**23**
Median time since admission until sample collection *(days, Min-Max)*	n.d.	3 (0-25)	1 (0-5)	2 (0-23)	11 (1-25)	14 (3-25)
Median duration of symptoms at sample collection *(days, Min-Max)*	n.d.	8 (0-30)	11 (5-21)	12 (4-28)	16 (4-32)	21 (12-32)
Median duration of symptoms at admission *(days, Min-Max)*	n.d.	8 (1-20)	9 (2-20)	8 (1-15)	7 (1-16)	6 (1-16)
Median Age *(years, Min-Max)*	52 (23-82)	61 (22-89)	61 (22-86)	58 (27-89)	61 (28-75)	61 (28-75)
Sex (% Male*)*	22.73%	57.8%	47.37%	57.14%	66.67%	61%
Clinical parameters *(Median, Min-Max)*						
Respiratory rate (rpm)	14 (12-20)	24 (12-49)	20 (12-26)	24 (14-40)	34 (20-49)	32 (15-49)
PaFiO2	438.09 (380.95-476.2)	233 (58-428.6)	328.09 (163.89-428.6)	228.57 (89-314.28)	146.25 (58-426)	114.8 (70-426)
Comorbidities (n,%)	2 missing					
Tobacco	4 (20%)	11 (17.46%)	0 (0%)	7 (35%)	4 (16.67%)	6 (26.09%)
Hypertension	3 (15%)	18 (28.13%)	3 (15.79%)	6 (28.57%)	9 (37.5%)	10 (43.48%)
Diabetes Mellitus	1 (5%)	12 (18.75%)	1 (5.26%	3 (14.29%)	8 (33.33%)	6 (26.09)
Dyslipidemia	3 (15%)	22 (34.48%)	4 (21.05%)	9 (42.86%)	9 (37.5%)	10 (43.48)
History of cardiovascular disease	0	9 (14.06%)	1 (5.26%)	3 (14.29%)	5 (20.83%)	5 (21.74%)
History of lung disease	3 (15%)	13 (20.31%)	4 (21.05%)	6 (28.57%)	3 (12.5%)	7 (30.43%)
Laboratory values *(Median, Min-Max)*						
Serum IL-6 (pg/ml)	1.5 (0-201)	14.86 (0-941.26)	3.69 (0-53.54)	16.41 (0-64.37)	49.8 (0-941.26)	47.4 (2.6-458.5)
PCT (ng/ml)	n.d.	0.11 (0.02-12.34)	0.06 (0.02-0.41)	0.12 (0.03-4.14)	0.18 (0.02-12.34)	0.18 (0.02-1.2)
CRP (mg/dl)	0.11 (0-0.42)	7.31 (0.32-63.6)	2.85 (0.32-16.57)	6.8 (1.19-28.5)	18.02 (0.47-63.6)	18 (0.47-63.6)
Glucose (mg/dl)	89 (69-142)	122 (73-327)	105 (77-174)	113 (73-190)	150 (79-327)	125 (95-327)
GGT (U/L)	13.5 (7-40)	62 (12-1743)	52 (15-247)	62 (14-1743)	63 (12-609)	60 (21-609)
Lymphocyte Count	2275 (1150-4710)	1030 (160-7200)	1230 (240-2310)	1060 (330-2930)	670 (160-7200)	980 (210-7200)
D-dimer (µg/ml)	n.d.	0.8 (0.22-42.1)	0.63 (0.24-5.66)	0.79 (0.31-6.68)	2.13 (0.22-42)	0.9 (42-0.3)

LDH (U/L)	154 (134-179)	300 (119-1319)	236 (119-236)	289 (184-474)	432 (244-1319)	448 (252-1319)
Ferritin (ng/ml)	72 (10-325)	1111 (124-8266)	753 (124-4234)	1097 (232-3474)	1555 (442-8266)	1000 (7468-274)
Intercurrent events						
Superinfection *n (%)*	0	19 (31.15%) 3 missing	0	2 (9.52%)	17 (80.95%) 3 missing	20 (100%) 3 missing
Treatment since admission until sample extraction *n (%)*	0	61 (95.31%)	16 (84.21%)	21 (100%)	22 (91.67%)	23 (100%)
Hidroxychloroquine		61 (95.31%)	16 (84.21%)	21 (100%)	22 (91.67%)	23 (100%)
Lopinavir/Ritonavir		50 (78.13%)	13 (68.42%)	17 (80.95%)	18 (75%)	19 (82.6%)
Azithromycin		55 (85.94%)	16 (84.21%)	17 (80.85%)	22 (91.66%)	21 (91%)
Ceftriaxone		31 (48.44%)	2 (10.53%)	10 (47.62%)	19 (79.16%)	15 (65%)
Other antibiotics		18 (28.57%)	0	4 (19.05%)	14 (58.33%)	20 (87%)
Glucocorticoids		35 (54.69%)	8 (42.11%)	8 (38.1%)	19 (79.17%)	21 (91%)
Tozilizumab		19 (29.69%)	0	3 (14.29%)	16 (66.67%)	18 (78%)

Supplemental Table 1. Demographic and clinical information from study patient cohorts.

	G2 Severe COVID-19	G3 Critical COVID-19 Blood	G3 Critical COVID-19 Bronch.
Number of patients *n, (%)*	**2 (9.52%)**	**17 (80.95%)**	**23 (100%)**
Median time since admission until ICU *(days (Min-Max))*	n.d.	0 (0-12)	3 (0-12)
Median duration of symptoms until ICU admission *(days (Min-Max))*	n.d.	10 (2-30)	11 (5-31)
Median time since ICU admission until culture extraction *(days (Min-Max))*	n.d.	6 (0-20)	6 (0-16)
Median PCT (ng/ml) *(Min-Max)*	0.12 (0.11-0.12)	0.22 (0.04-12.34)	0.2 (0.03-1.2)
ICU *n, (%)*	0	16 (94.1%)	23 (100%)
IMV *n, (%)*	0	**15 (88.24%)**	23 (100%)
NO IMV n, (%)	2 (100%)	**2 (11.76%)**	0
Type of superinfection in patients receiving IMV *n, (%)*			**3 missing**
Bacterial	n.d.	10 (66.66%)	13 (65%)
Fungal	n.d.	4 (26.66%)	6 (30%)
Both	n.d.	1 (6.66%)	1 (5%)
Type of superinfection in patients not requiring IMV *n, (%)*			
Bacterial	2 (100%)	2 (100%)	n.d.
Fungal	0	0	n.d.
Both	0	0	n.d.
Organ of superinfection *n, (%)*			**3 missing**
Lung	1 (50%)	9 (52%)	11 (55%)
Peripheral blood	1 (50%)	3 (18%)	4 (20%)
Urinary	0	3 (17%)	2 (10%)
Two organs	0	2 (11%)	3 (15%)

Supplemental Table 2. Detection of microbial superinfection in severe and critical COVID-19 patients.

Antibody	Ref	Clone	Fluorochrome	Source
CD40	334306	5C3	FITC	BioLegend
CD38	340909	HB-7	FITC	BioLegend
CD14	367104	63D3	PE	BioLegend
CXCR5	356903	J252D4	PE	BioLegend
CD141	344106	M80	APC	BioLegend
HLA-DR	347403	L243	APC	BD
CD123	560087	7G3	APC	BD
CD19	363016	SJ25C1	PerCP-Cy5.5	BioLegend
CD3	300328	HIT3a	PerCP-Cy5.5	BioLegend
CD56	362526	5.1H11	PerCP	BioLegend
CD20	332781	L27	PerCP-Cy5.5	BD
CD1c	331516	L161	PE-Cy7	BioLegend
CD16	302021	3G8	PB	BioLegend
CD11c	301626	3.9	PB	BioLegend
CD3	3cFB1-100T	33-2A3	PB	Immunostep
HLA-DR	307618	I.243	APC-Cy7	BioLegend
CD8	300925	HIT8a	APC-Cy7	BioLegend
CD45	560777	HI30	PO	BD

Supplemental Table 3. Commercial antibodies used for flow cytometry analysis in the study.

Supplemental Figure 1

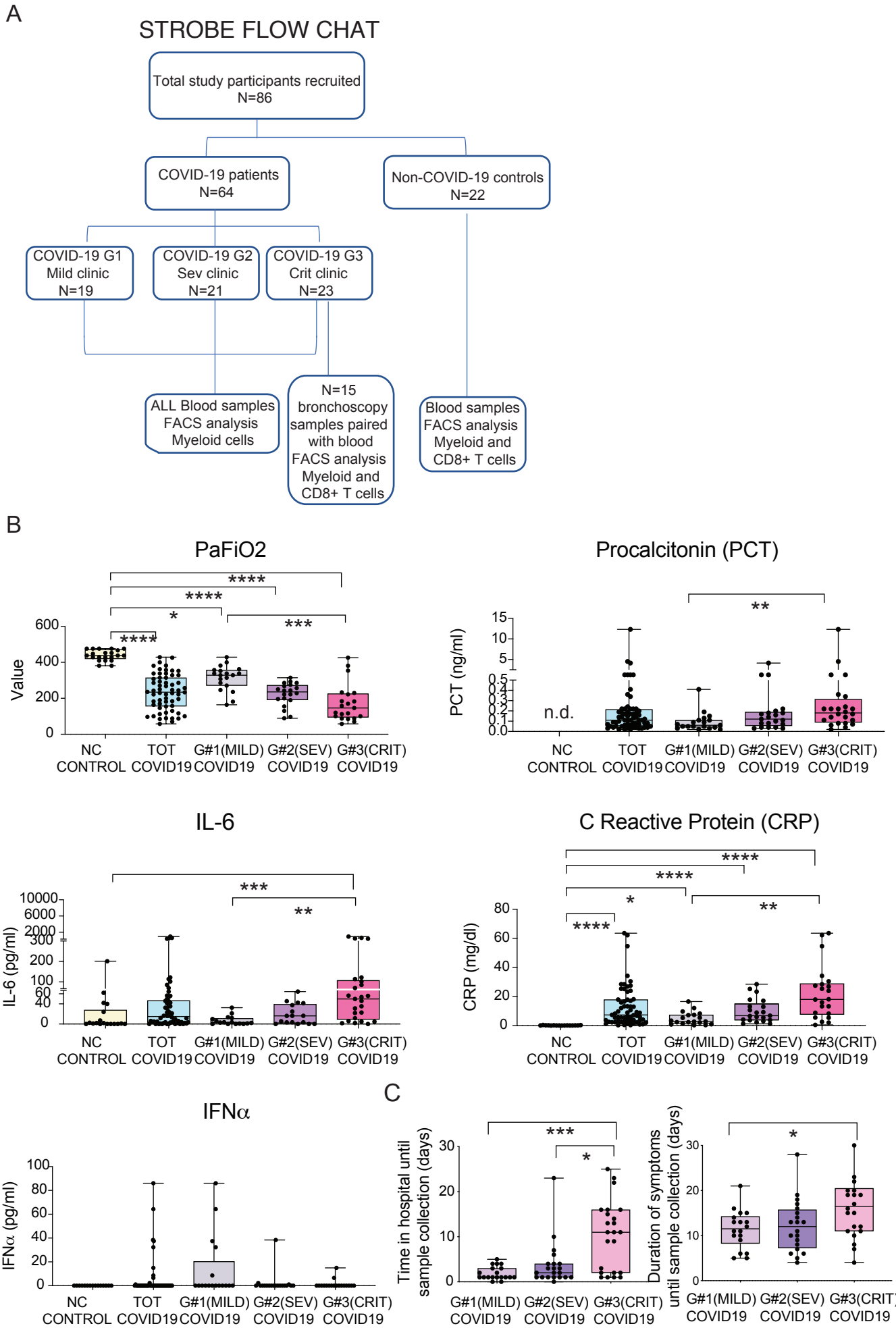

Supplemental Figure 1. Selected clinical parameters differentially detected in subgroups of COVID-19 patients with different clinical severity. (A): STROBE Flow chart of the study showing patient recruitment and stratification according to clinical severity (B): Box and Whiskers plots representing clinical values of PaFiO2, IL-6, procalcitonin, IFNα and C Reactive Protein detected in the blood of total number of COVID-19 patients or patients stratified into mild (G1; n=19), severe (SEV, G2; n=21) and critical (CRIT, G3; n=24) clinical status defined according to the criteria detailed in Supplemental Table 1. Values present in non-COVID-19 controls (NC; n=22) were included when available. Error bars represent maximum and minimum values. Statistical significance of differences in clinical values across the study groups were calculated using a Kruskal wallis and Dunn´s post-hoc test for multiple comparisons. *p<0.05; **p<0.01; ***p<0.001; ****p<0.0001. (C): Time since hospital admission (left) and symptoms duration (right) at the time of sample collection for the three mentioned subgroups of COVID-19 patients. Statistical significance was calculated using a Kruskal Wallist and Dunn´s post-hoc tests. *p<0.05; ***p<0.001.

Supplemental Figure 2

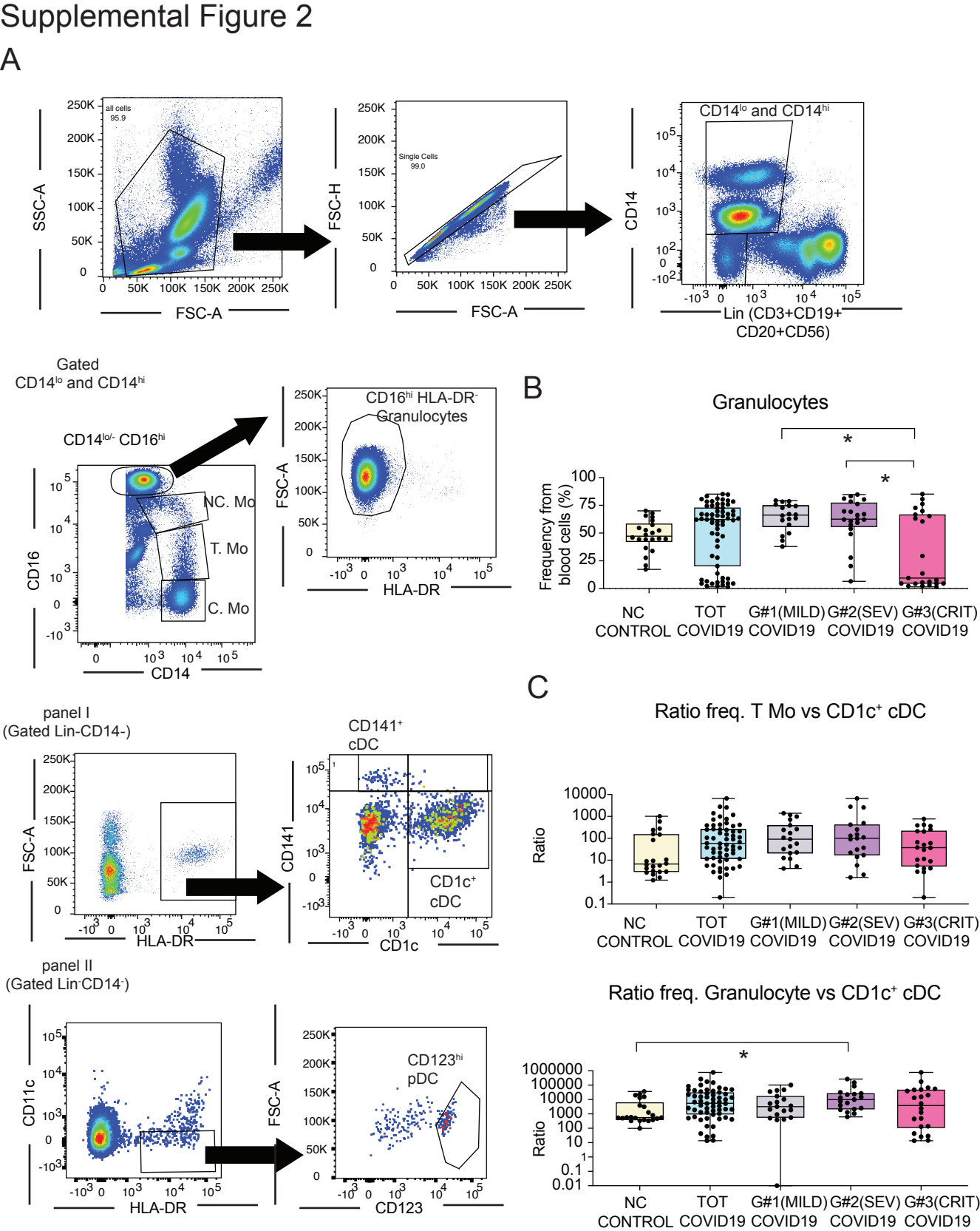

Supplemental Figure 2. Flow cytometry characterization of myeloid cell subsets from COVID-19 patients. (A): Flow cytometry gating strategy showing Monocyte (Mo), conventional (cDC) and plasmacytoid DC (pDC) and granulocyte characterization in the blood from a representative patient of our study cohorts. CD14+ Lineage (CD3- CD19- CD20- CD56-) negative Mo subsets were defined by CD14 and CD16 expression levels. Granulocytes were identified as large CD16hi CD14lo/- HLADR- cells. cDC subsets were identified as CD14- Lin- HLA-DR+ big cells differing on CD1c and CD141 expression. Finally, pDCs were defined as CD14-Lin-CD11c- HLADR+ CD123hi lymphocytes. (B-C): Box and whiskers plots reflecting proportions of granulocytes (B) and ratios of frequencies between Transitional Mo/CD1c+ cDC and Granulocyte/ CD1c+ cDCs (C) present in the blood of non-COVID-19 control individuals (n=22) compared with either total COVID-19 patients included in the study or patients stratified into mild (G1; n=19), severe (SEV, G2; n=21) and critical (CRIT, G3; n=24). Error bars represent maximum and minimum values. Statistical differences between patient groups were calculated using a Kruskal Wallis test followed by a Dunn´s post hoc-test for multiple comparisons. *p<0.05.

Supplemental Figure 3

A

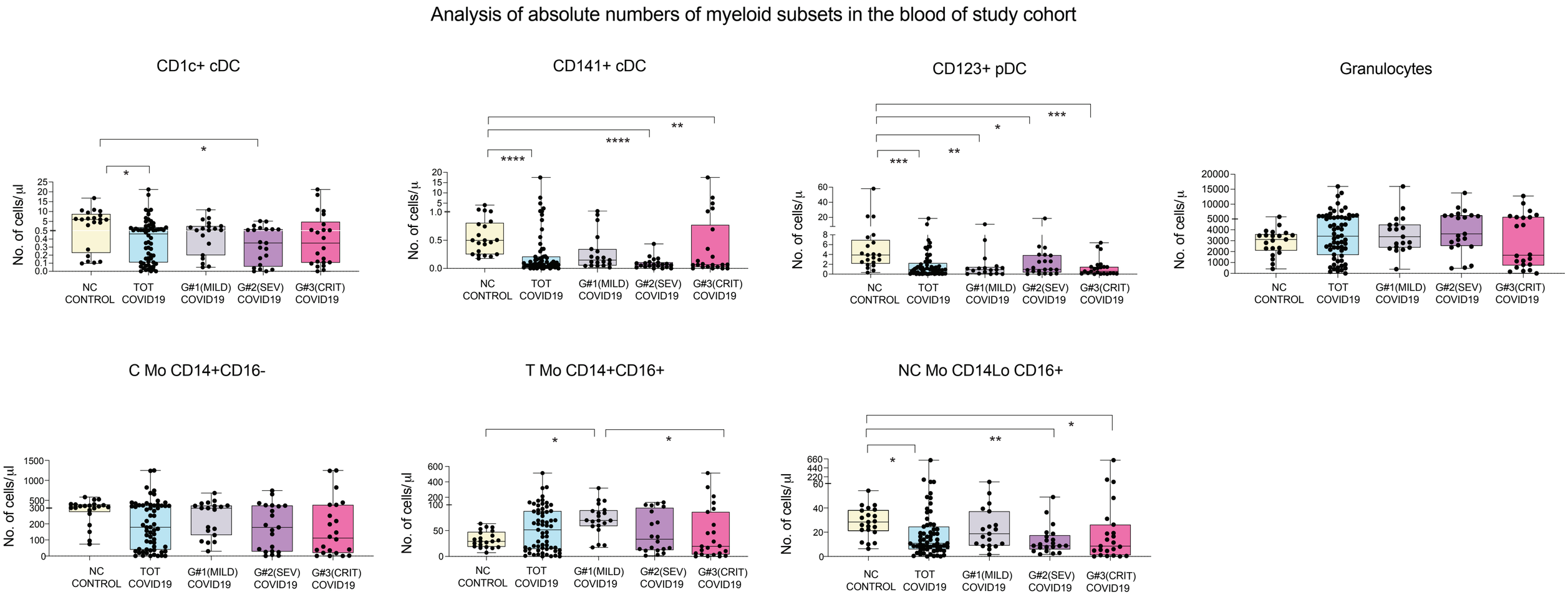

B

Supplemental Figure 3. Analysis of Absolute numbers of myeloid subsets in COVID-19 cohort groups and stratification of critical patients based on microbial superinfection. (A-C): Box and Whiskers plots representing absolute numbers of indicated myeloid cell populations present in the blood of non-COVID-19 (NC; n=22) control individuals versus either total COVID-19 patients included in the study or patients stratified into groups according to mild (G1; n=19), severe (SEV, G2; n=21) and critical (CRIT, G3; n=22) clinical status as shown in Supplemental Table 1. Median of values is shown. Error bars represent maximum and minimum values. (B) Box and Whiskers plots representing relative (left plots) and absolute (right plots) numbers for all cell populations from NC controls versus total critical G3 COVID-19 patients or stratified based on the presence of microbial superinfection (Sup. Inf) in the lung (n=8), both lung and blood (Bd) or unine (Ur) (n=2), or only in Bd/Ur (n=6) or that did not present super infection (No Sup. Inf; n=4). Median of values is shown. Error bars represent maximum and minimum values. Statistical significance of differences between all patient groups (A) or COVID-19 patients compared to non-COVID-19 controls (NC) in (B) was calculated using a Kruskal Wallis test followed by a Dunn´s post hoc-test for multiple comparisons. *p<0.05; **p<0.01; ***p<0.001; ****p<0.0001.

Supplemental Figure 4

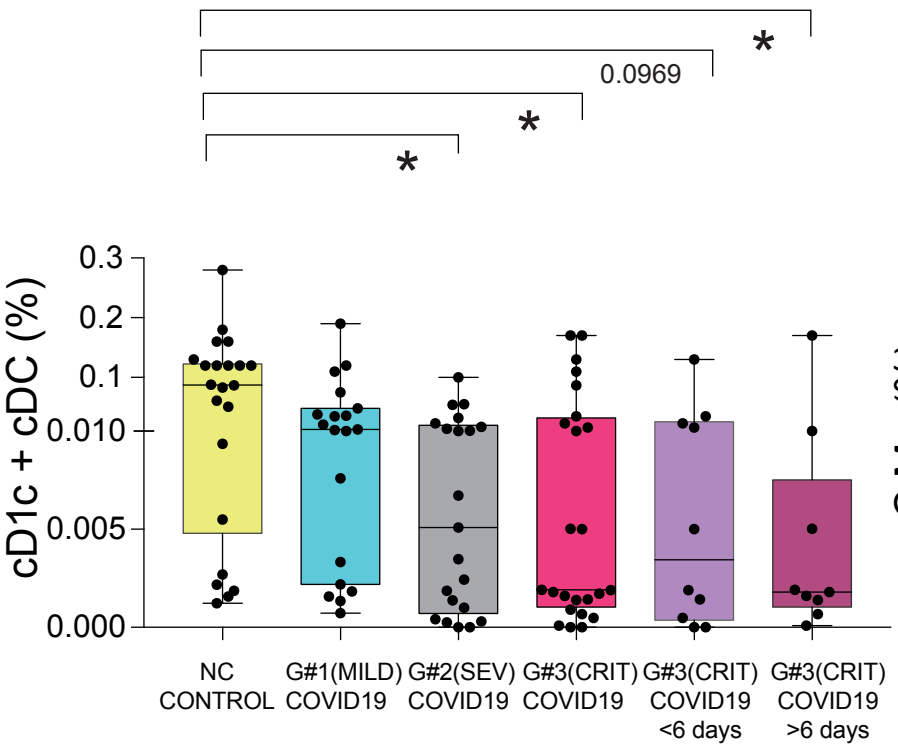

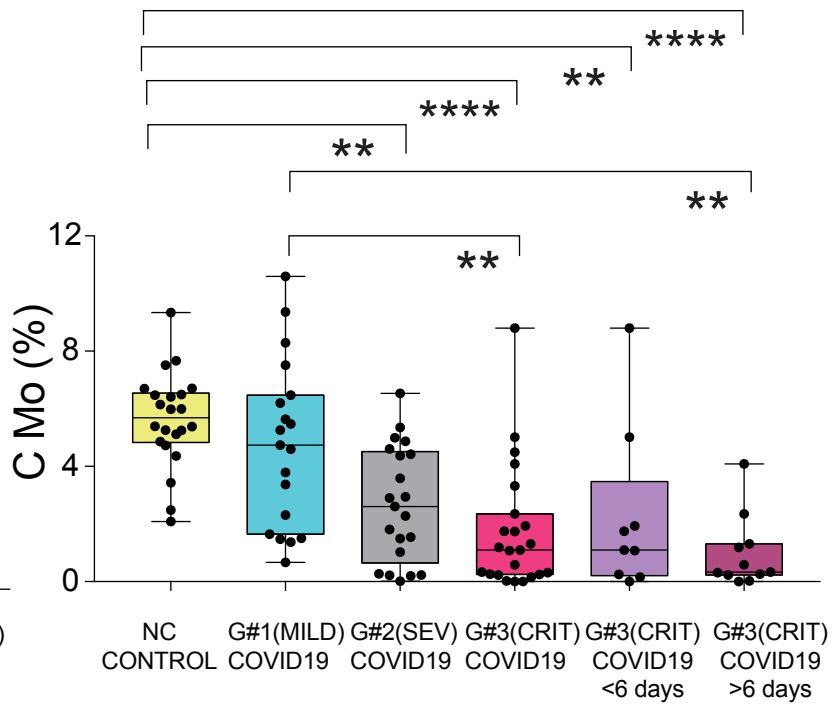

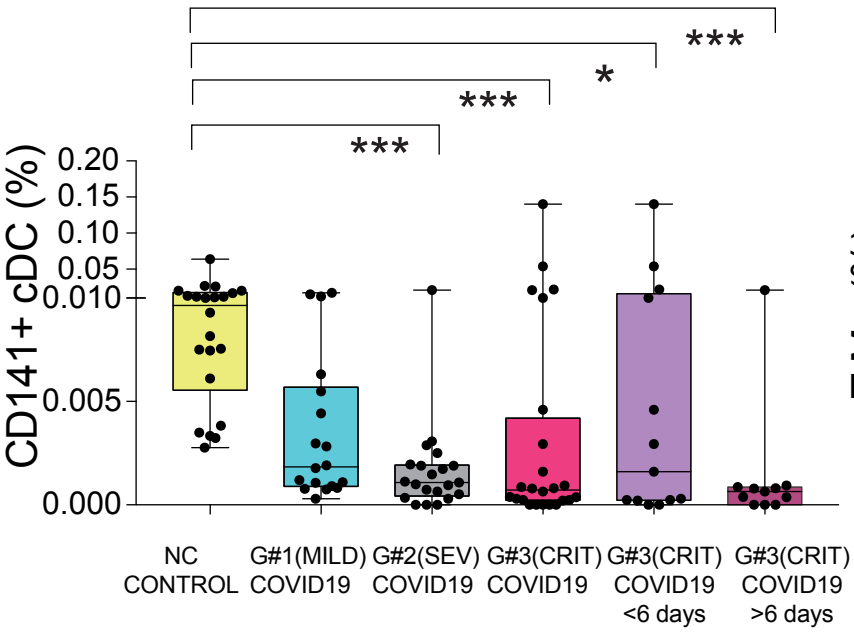

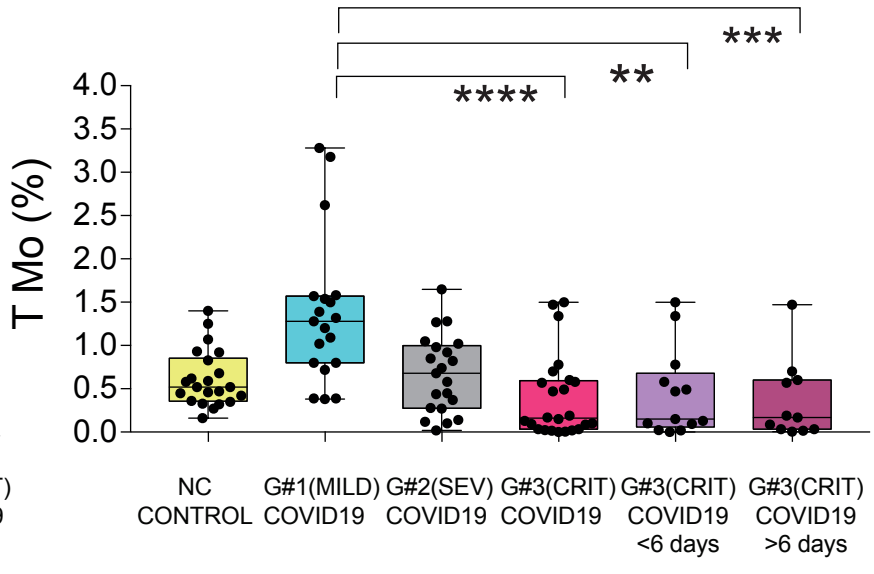

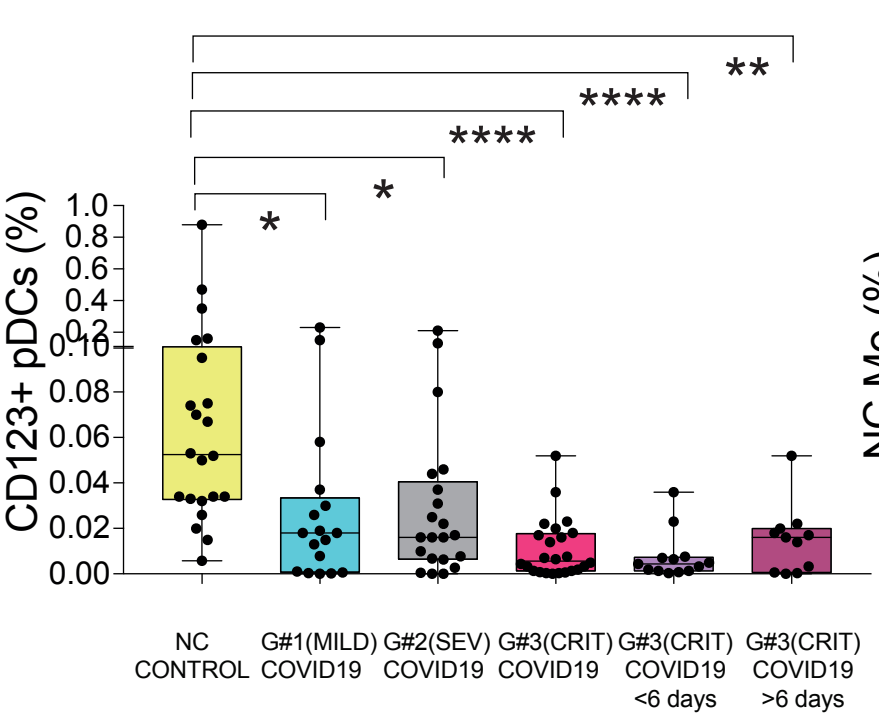

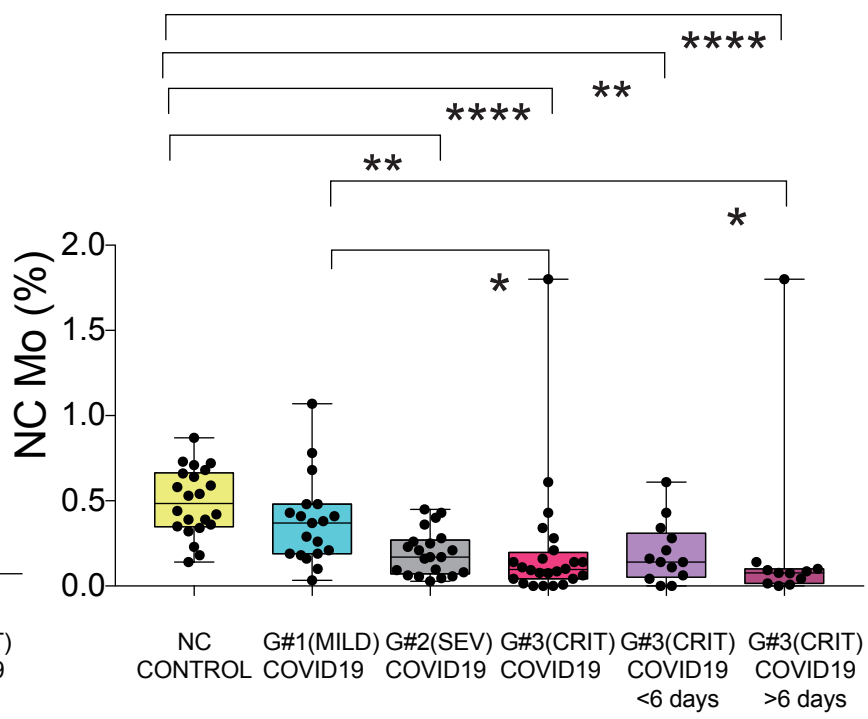

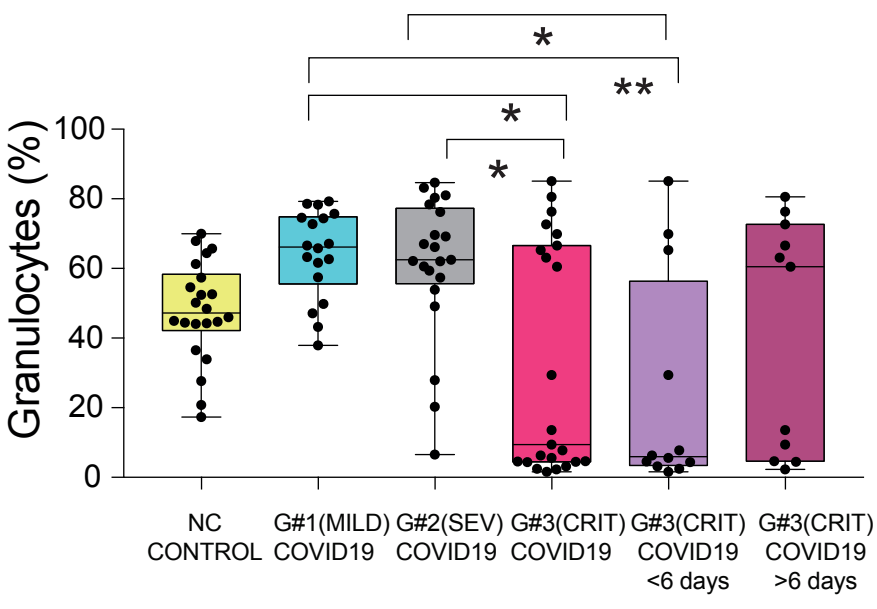

Supplemental Figure 4. Analysis of frequencies of circulating myeloid subsets in COVID-19 after stratification of critical patients based on days at ICU. Box and whiskers plots reflecting frequencies of the indicated circulating myeloid subsets in critical G3 COVID-19 patients stratified by time since hospital admission (< 6 days, n=13; > 6 days, n=11) and compared to mild (G1; n=19), severe (SEV, G2; n=21) and total critical (CRIT, G3; n=24) patients. Error bars represent maximum and minimum values. Statistical significance of differences between patient groups was calculated using a Kruskal Wallis test followed by a Dunn´s post hoc-test for multiple comparisons. *p<0.05; **p<0.01; ***p<0.001; ****p<0.0001.

Supplemental Figure 5

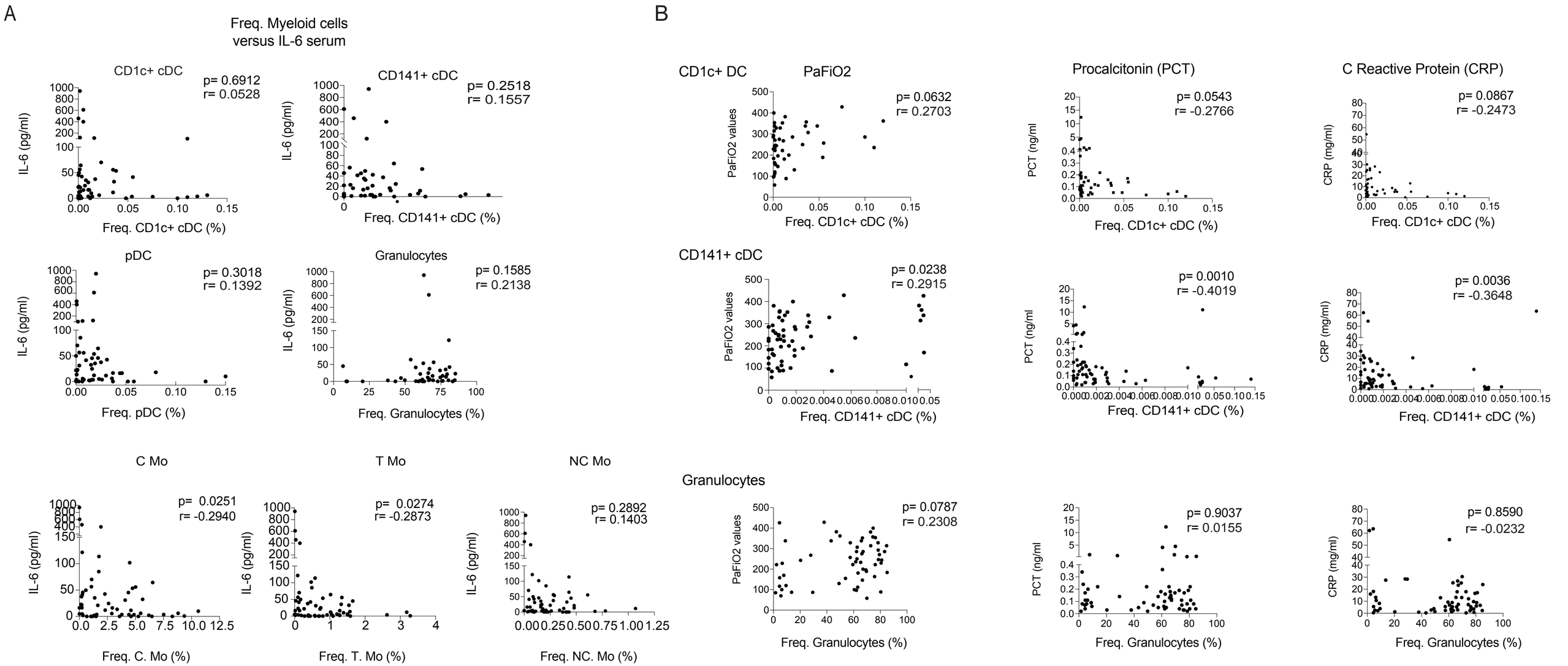

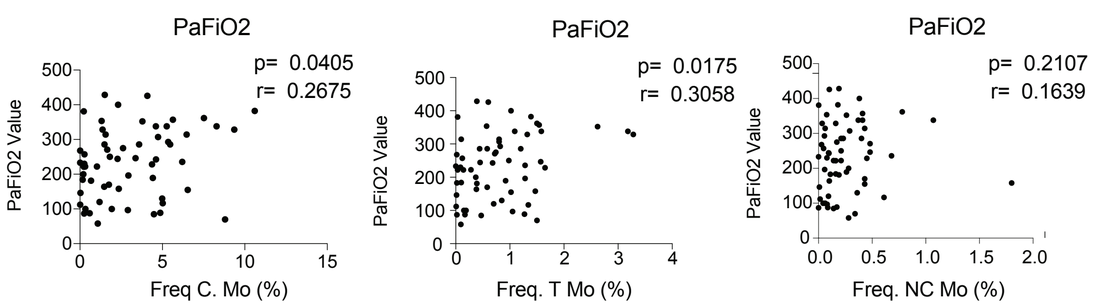

Supplemental Figure 5. Correlation of frequencies of circulating myeloid cell subsets with IL-6 and inflammatory marker plasma levels. Spearman correlations between IL-6 plasma levels (A) or inflammatory clinical values (B-C) and percentages of the indicated myeloid cell subsets in the blood of COVID-19 patients. Spearman P and R values are shown in the upper right corner of the plot.

Supplementary Figure 6

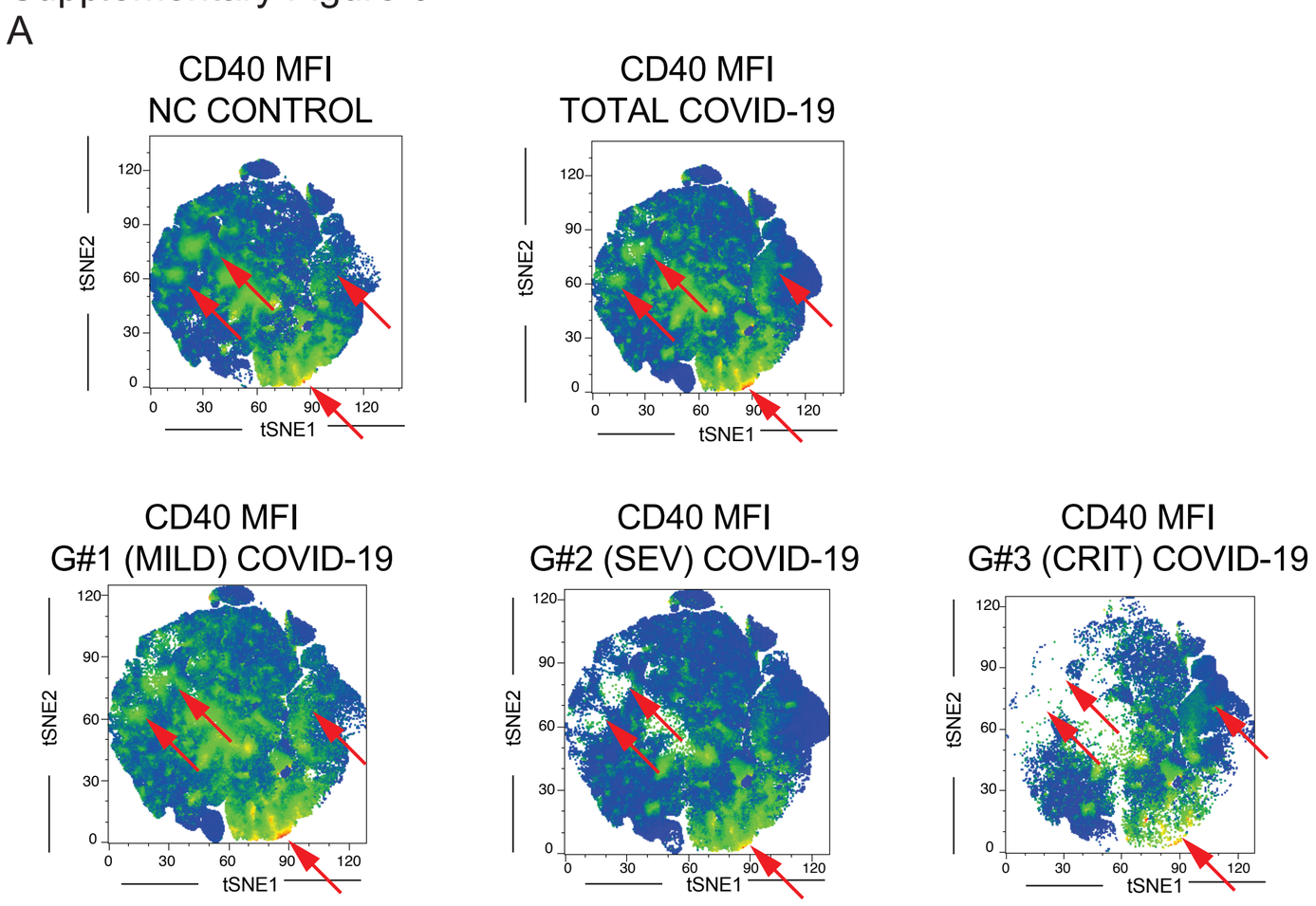

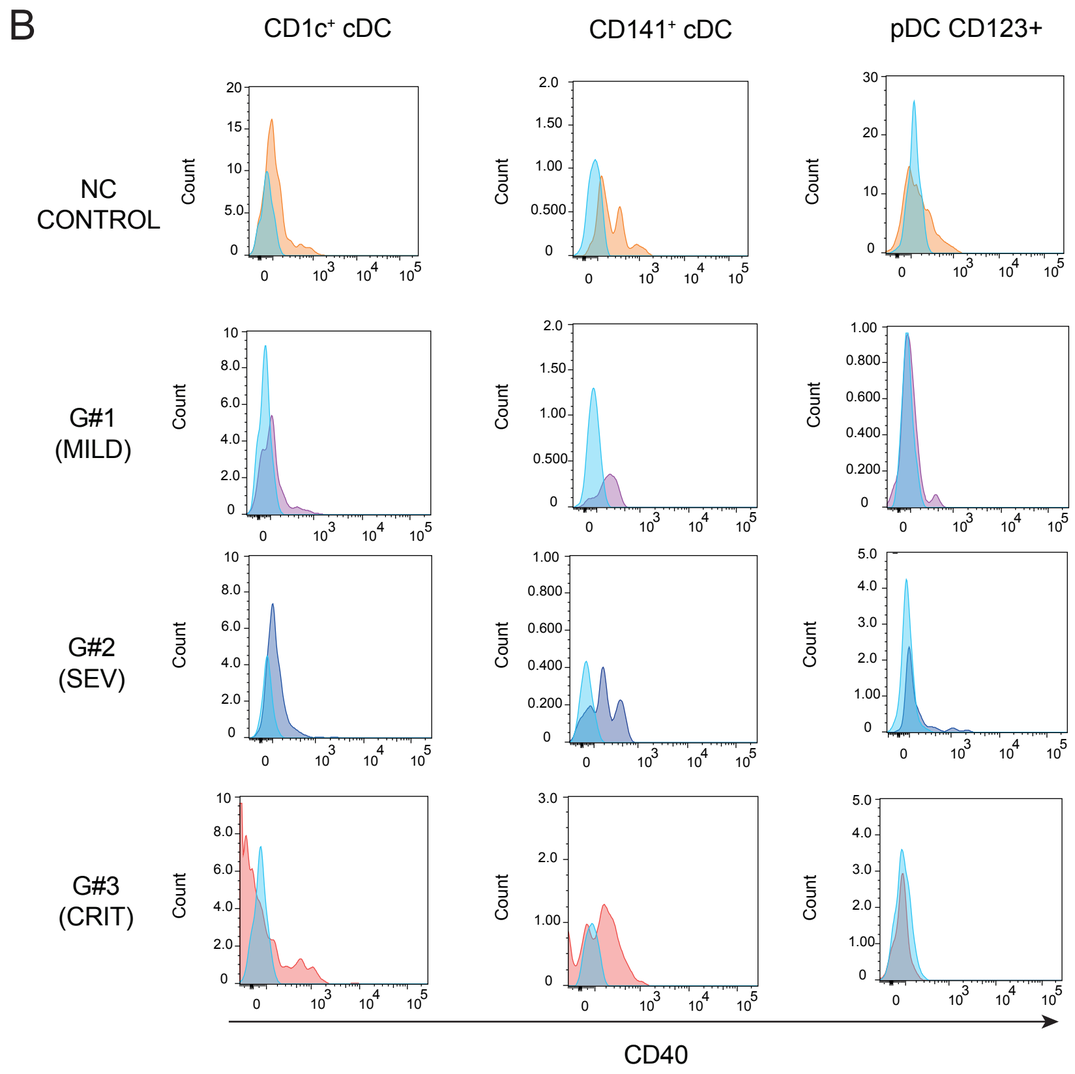

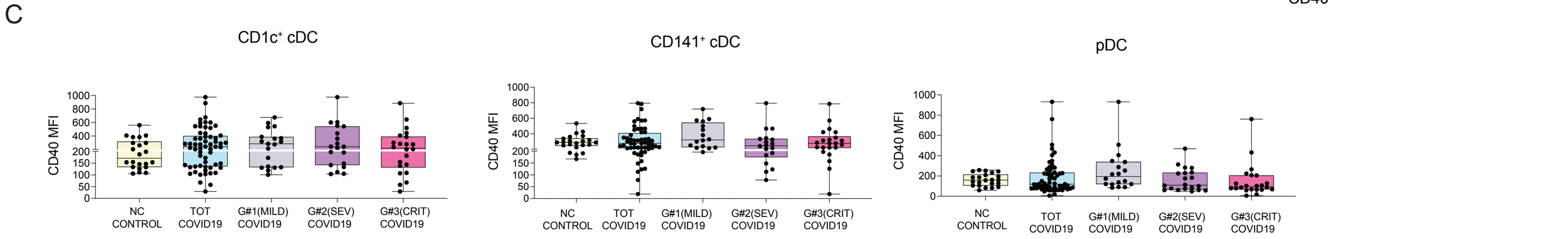

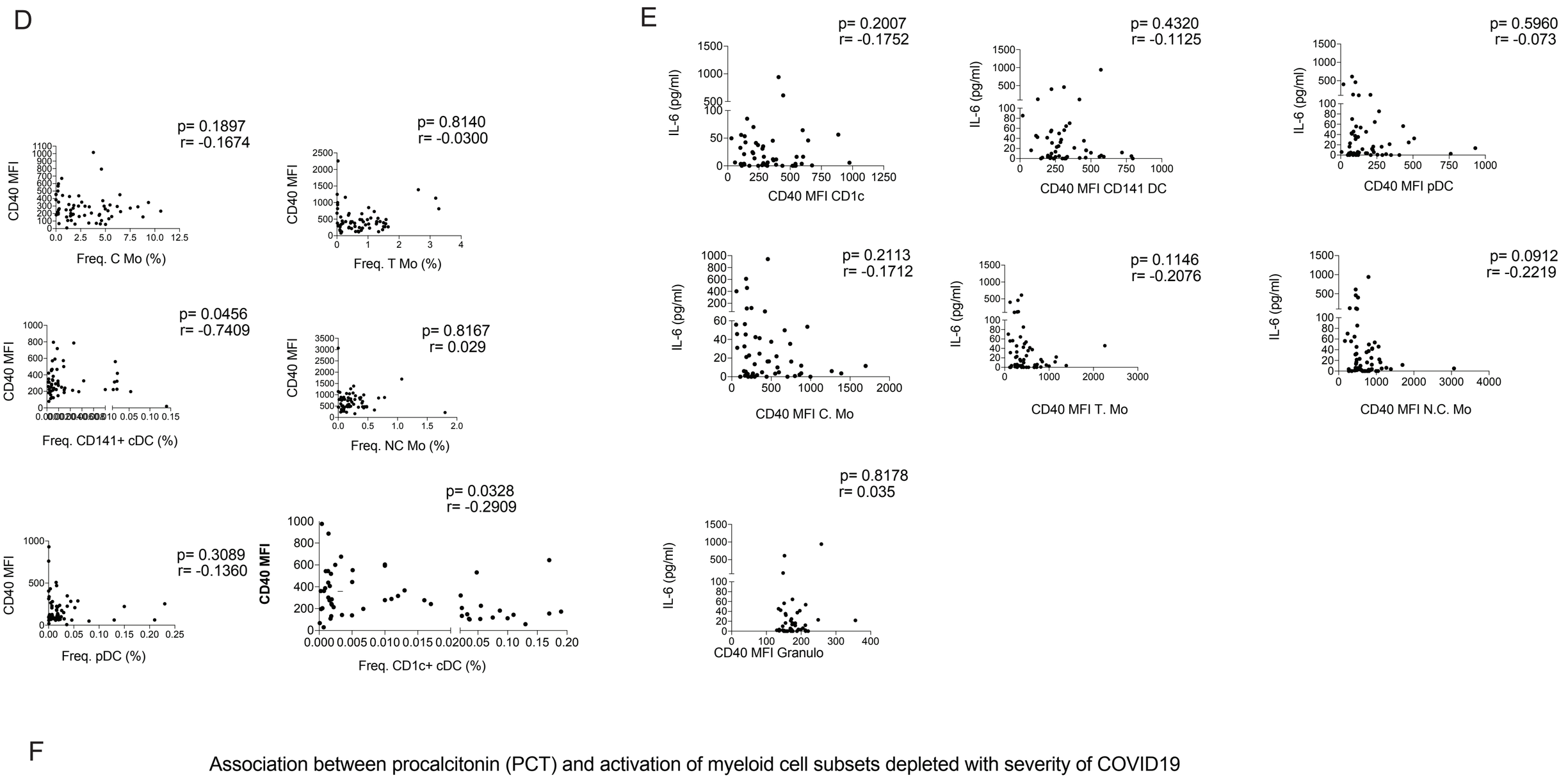

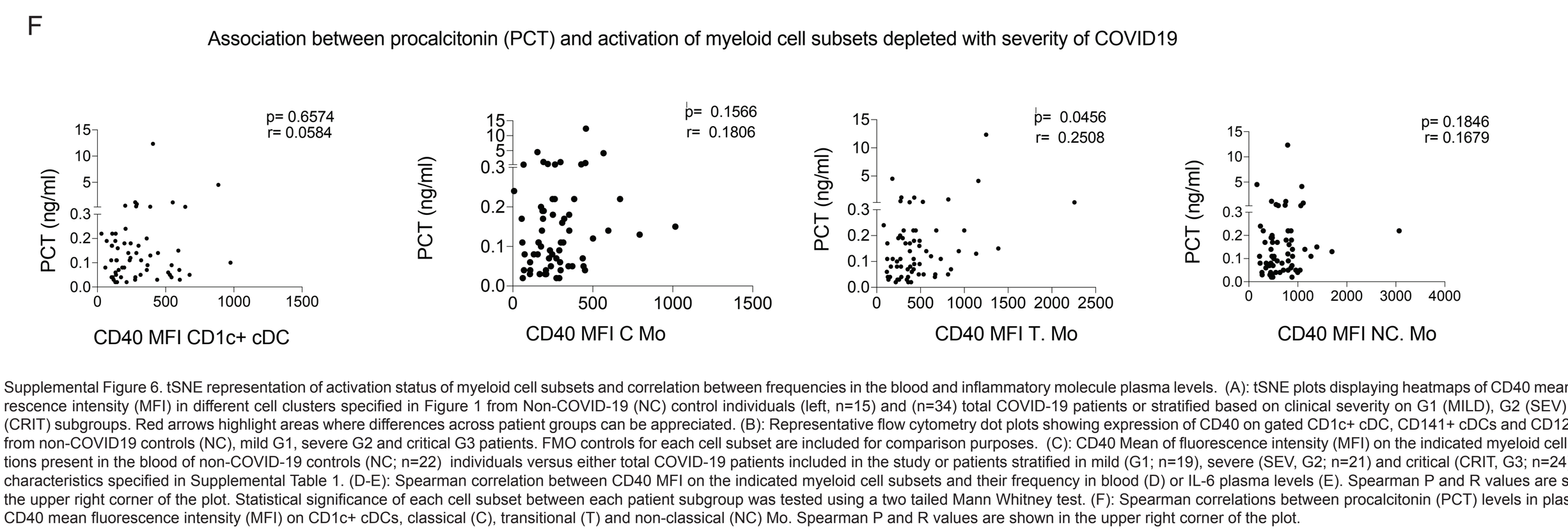

Supplemental Figure 6. tSNE representation of activation status of myeloid cell subsets and correlation between frequencies in the blood and inflammatory molecule plasma levels. (A): tSNE plots displaying heatmaps of CD40 mean of fluorescence intensity (MFI) in different cell clusters specified in Figure 1 from Non-COVID-19 (NC) control individuals (left, n=15) and (n=34) total COVID-19 patients or stratified based on clinical severity on G1 (MILD), G2 (SEV) and G3 (CRIT) subgroups. Red arrows highlight areas where differences across patient groups can be appreciated. (B): Representative flow cytometry dot plots showing expression of CD40 on gated CD1c+ cDC, CD141+ cDCs and CD123+ pDC from non-COVID19 controls (NC), mild G1, severe G2 and critical G3 patients. FMO controls for each cell subset are included for comparison purposes. (C): CD40 Mean of fluorescence intensity (MFI) on the indicated myeloid cell populations present in the blood of non-COVID-19 controls (NC; n=22) individuals versus either total COVID-19 patients included in the study or patients stratified in mild (G1; n=19), severe (SEV, G2; n=21) and critical (CRIT, G3; n=24) clinical characteristics specified in Supplemental Table 1. (D-E): Spearman correlation between CD40 MFI on the indicated myeloid cell subsets and their frequency in blood (D) or IL-6 plasma levels (E). Spearman P and R values are shown in the upper right corner of the plot. Statistical significance of each cell subset between each patient subgroup was tested using a two tailed Mann Whitney test. (F): Spearman correlations between procalcitonin (PCT) levels in plasma and CD40 mean fluorescence intensity (MFI) on CD1c+ cDCs, classical (C), transitional (T) and non-classical (NC) Mo. Spearman P and R values are shown in the upper right corner of the plot.

Supplemental Figure 7

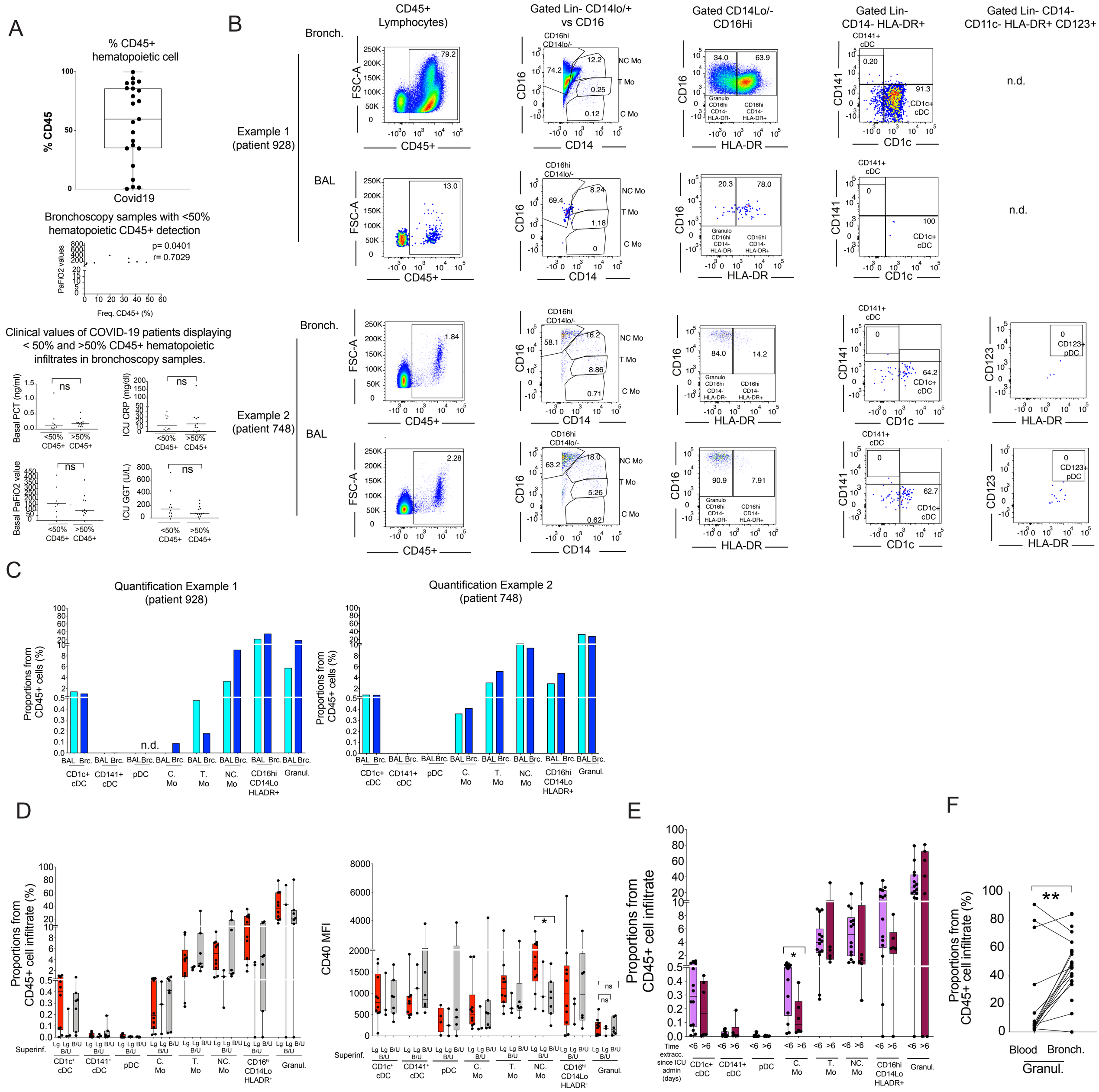

Supplemental Figure 7. Characterization of myeloid cells present in bronchoscopy infiltrates from COVID-19 patients with ARDS. (A): Dot plots representing proportions of CD45+ hematopoietic cells present in bronchoscopy samples obtained from COVID-19 patients (n=23) with severe ARDS and requiring IMV at hospital´s ICU. Associations with clinical parameters in samples with frequencies of CD45+ hematopoietic cell superior or inferior to 50% are shown below. Median values are highlighted with a line. (B): Flow cytometry analyses of myeloid cell subsets hematopoietic infiltrates from bronchoscopy compared with bronchoalveolar lavage (BAL) from the same COVID-19 severe patient. Two representative examples are shown. (C): Quantification of proportions of the indicated myeloid population in the BAL and bronchoscopy (Brc.) from the two patients shown in (B). (D-E): Box and Whiskers plots representing percentages (D,left) and CD40 Mean of Fluorescence Intensity (MFI D, right) corresponding to the indicated cell populations in the hematopoietic CD45+ infiltrate present in bronchoscopy mucus samples from severe COVID-19 patients (n=20) presenting ARDS and receiving IMV at ICU and stratified by detection of microbial superinfection only in the lung (Lg; n=10), both in lung and Blood or Urine (Lg+B/U, n=3) or only in the blood or urine (B/U; n=7) or time of sample collection since ICU admission (E) (< 6 days, n=14; > 6 days; n=6). Median are highlighted and error bars represent maximum and minimum datapoint. Statistical differences between proportions of cell populations within the same infiltrates were calculated using a two-tailed matched pairs Mann Whitney test and Bonferroni multiple comparison correction. (F): Frequencies of CD14lo/- CD16hi HLA-DR- granulocytes on the blood and paired bronchoscopy samples from critical COVID-19 patients. Statistical differences were calculated using a two-tailed matched pairs Wilcoxon test. **, p<0.01; ***;p<0.001.

Supplemental Figure 8

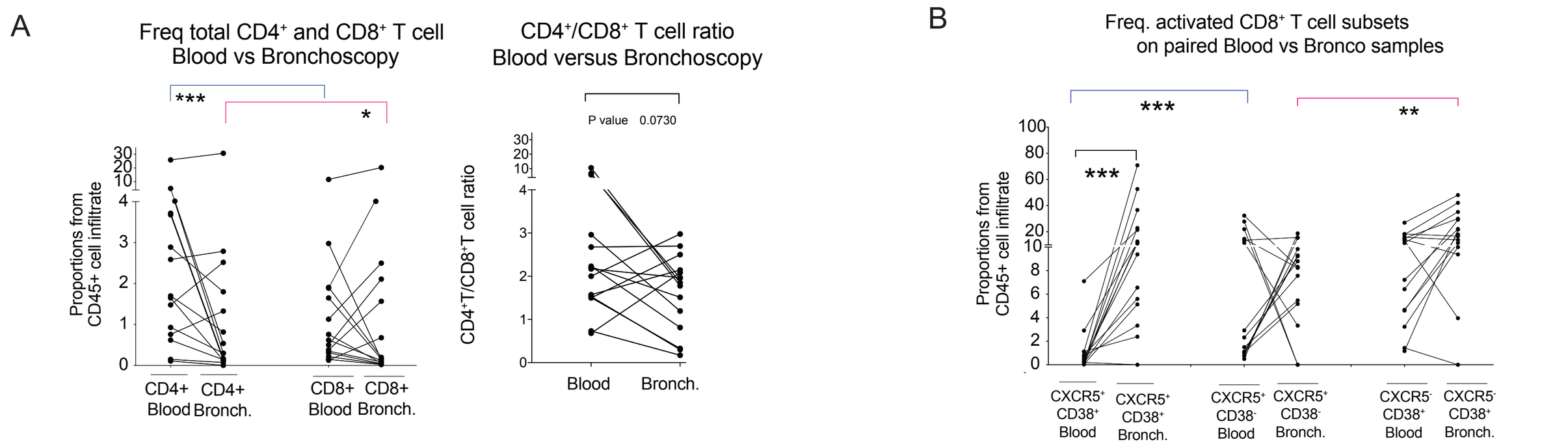

Supplemental Figure 8. Characterization of effector CD8+ T cells present in bronchoscopy infiltrates from COVID-19 patients with ARDS. (A-B): Percentages of total CD4+ and CD8+ T cells and CD4+T/CD8+T ratios (A) or CXCR5+CD38+ (DP), CXCR5+ CD38- (CXCR5SP) and CXCR5- CD38+ (CD38SP) (B) from CD8+ T cells in the blood and paired bronchoscopy samples from n=15 COVID-19 patients with ARSD (n=15). Statistical significance was calculated using a two tailed matched pairs Wilcoxon test for differences of the same populations between different tissue localizations (black) or between different cell populations included within the blood (blue) or within the bronchoscopy (pink) samples. (C-D): Spearman correlations between proportions of CXCR5+CD38+, CXCR5+ CD38- and CXCR5- CD38+ subpopulations of CD8+ T cells from bronchoscopy samples from COVID-19 patients and ratios of frequencies between Transitional (T) or non-classic (NC) Mo versus CD1c+ cDCs (C) and CD40 MFI of the indicated myeloid populations in bronchoscopy samples (D). Spearman P and R values are shown in the upper right corner of the plot.